The role of a weakened Atlantic meridional overturning circulation in modulating marine heatwaves in a warming climate

Xianglin Ren[1] and Wei Liu[1]

[1]Department of Earth and Planetary Sciences, University of California Riverside, Riverside, CA, USA

Corresponding author: Wei Liu (wei.liu@ucr.edu)

Key Points:

- A. The AMOC slowdown has an insignificant effect on global MHWs over the past four decades except those at the NAWH.
- B. The effect of the AMOC on MHWs will become significant in broad areas in the North Atlantic and North Pacific by the end of current century.
- C. The NAWH region would reach a near-permanent MHW state over 2061-2100 without a slowdown of the AMOC.

Abstract

We explore the effect of Atlantic meridional overturning circulation (AMOC) slowdown on global marine heatwaves (MHWs) under anthropogenic warming by maintaining AMOC strength in climate model simulations throughout the twenty-first century. The AMOC slowdown has an insignificant effect on global MHWs during the past four decades, except those over the North Atlantic warming hole (NAWH) where the weakened AMOC reduces the occurrence and duration of MHWs by about half by creating a cooler mean-state sea surface temperature. As the AMOC continues weakening in current century, its effect becomes significant on MHWs in the North Atlantic and Pacific Oceans. The weakened AMOC induces a bipolar-seesaw like change in MHW frequencies, with more frequent MHWs in the Southern Hemisphere, but less frequent MHWs in the North Hemisphere except over the NAWH. The reason for the exception is that the NAWH region would enter a near-permanent MHW state without an AMOC slowdown.

Plain Language Summary

In this study, we examine how the weakened Atlantic meridional overturning circulation (AMOC) affects global MHWs under greenhouse gas warming. We conduct a climate model experiment by keeping AMOC magnitude constant throughout the twenty-first century and compare this experiment with a parallel AMOC weakening case. We find that the AMOC effect on MHWs is insignificant over most of global oceans during the past four decades. The only exception happens to a region to the south of Greenland that is so-called the North Atlantic warming hole (NAWH). The weakened AMOC creates a cooler mean-state sea surface temperature in this region than the others, which helps reduce the occurrence and duration of MHWs there. Since the magnitude of AMOC weakening is expected to be larger as time goes on, the AMOC effect on MHWs will become significant later in the twenty-first century, especially in the North Atlantic and North Pacific. The weakened AMOC will make MHWs more frequent in the Southern Hemisphere, but less frequent in the North Hemisphere except in the NAWH region. The reason for the exception is that, if the AMOC were not to slow down, MHWs would occur in the NAWH region almost all year round.

1. Introduction

Marine heatwaves (MHWs) are characterized by prolonged periods of extreme warm sea surface temperatures (SSTs). During past two decades, several prominent MHWs have been reported in various regions of world's ocean, such as those in the Mediterranean Sea in 2003 (Garrabou et al., 2009) and 2006 (Bensoussan et al., 2010), off Western Australia in 2011 (Feng et al., 2013; Benthuysen et al., 2014), the Northwest Atlantic in 2012 (Mills et al., 2013; Chen et al., 2014, 2015), in the Tasman Sea in 2015–2016 (Oliver et al., 2017), in the East China Sea in 2016 (Tan & Cai, 2018) and in the Northeast Pacific in 2013–2015 (Bond et al., 2015; Di Lorenzo & Mantua, 2016) and 2019 (Amaya et al., 2020). These extreme events have caused substantial impacts on marine ecosystems (Peterson et al., 2017; Krumhardt et al. 2017; Smale et al., 2019) and socio-economically important fisheries (Pershing et al., 2015; Greene, 2016). Understanding the causes of such extreme events and unraveling the underlying dynamics, thereby, is of central importance for adaptation and sustainability under rapid climate change (Oliver et al., 2019).

Multiple physical drivers have been suggested to produce MHWs on various spatio-temporal scales (Holbrook et al., 2019, 2020; Oliver et al., 2021). For instance, persistent blocking highs over ocean and associated local air–sea interactions and feedbacks have been indicated as the trigger of the MHW events in the Northeast Pacific and Northwest Atlantic (Bond et al., 2015; Schlegel et al., 2021). The Madden–Julian Oscillation and El Niño-Southern Oscillation are important to the generation of the MHWs in the Indo-Pacific Oceans on intraseasonal and interannual timescales, respectively (Maloney & Kiehl, 2002; Jacox et al., 2016; Holbrook et al. 2021). On decadal timescales, the North Pacific Gyre Oscillation, North Atlantic Oscillation, Pacific Decadal Oscillation and Atlantic Multidecadal Oscillation could significantly modulate the MHWs in the Pacific and Atlantic Oceans (Di Lorenzo & Mantua, 2016; Scannell et al., 2016; Oliver et al., 2018).

Beyond above physical drivers, however, one gap remains in our understanding of the physics of MHWs: the role of the long-term weakening of the Atlantic meridional overturning circulation (AMOC). As a vital ocean circulation system, the AMOC has been found in a weakening state during the past several decades from RAPID array measurements and satellite altimetry (Frajka-Williams, 2015; Smeed et al., 2018). The AMOC weakening is even evident since the middle-to-late last century based on multi-proxy reconstructions (Rahmstorf et al., 2015; Thornalley et al., 2018) during the past millennium. While whether this deceleration of the Atlantic overturning is already happening remains debatable, these direct and indirect observations raise the possibility of a rapid AMOC slowdown (Weaver et al., 2012) or even shutdown (Liu et al., 2017) in the near future, as supported by state-of-art climate model projections (Figure S1a). The centurial AMOC slowdown could impose global impacts on various climate components in the Earth's system (Liu et al., 2020). Nevertheless, the role of this long-term AMOC slowdown in global MHWs has yet been found, which thus serves as the focus of this study.

2. Data and Methods

2.1. Observations and model simulations

We use the Daily Optimum Interpolation Sea Surface Temperature (OISST) version 2.1 (v2.1) from the National Oceanic and Atmospheric Administration (Banzon et al., 2020; Huang et al., 2021a,b). The data have a spatial resolution of 0.25°×0.25° and are available since September 1, 1981. We adopt OISST data from 1982 to 2019 to examine the observed MHWs over global oceans.

We employ a fully coupled climate model, the National Center for Atmospheric Research Community Climate System Model version 4 (CCSM4) of a norminal 1-degree resolution (Gent et al., 2011) that consists of the Community atmosphere Model version 4, the Community Land Model version 4, the sea ice component version 4, and the Parallel Ocean Program version 2. We use CCSM4 historical and Representative Concentration Pathway 8.5 (RCP8.5) simulations with five ensemble members (AMOC_free thereafter). By defining the AMOC strength as the maximum of the annual mean stream function below 500 m in the North Atlantic, we find CCSM4 simulates an AMOC slowdown since the 1980s under the historical and RCP8.5 scenarios, as consistent with many other climate models (Figure S1a,b). Parallel to the AMOC_free simulation, we conduct a sensitivity experiment (AMOC_fx thereafter) using CCSM4 with five ensemble members in which freshwater is extracted from the North Atlantic deep-water formation region (Figure 1c) such that the AMOC strength is well maintained in a warming climate throughout the twenty-first century (experimental setup detalied in Liu et al., 2020). The difference between the AMOC_free and AMOC_fx simulations reveals the climate impact of AMOC slowdown.

2.2. Detection of marine heatwaves

Based on Hobday et al. (2016), a MHW is defined as an event in which daily SST exceeds the local seasonal threshold (i.e., the 90th percentile of daily SST for the same day during the climatology period) for at least 5 consecutive days within a given sea area. Two events with an interruption of less than 3 days are considered as one MHW event. In this study, we delve into the MHWs during the past four decades as well as the last four decades of the current century, so the climatological periods for MHW detection are 1981-2020 and 2061-2100, respectively. For either reference period, the daily SST climatology and the 90th percentile threshold corresponding to each day are calculated from the AMOC_free simulation using the daily SST for all years within 11 days centered on that day, and the results obtained are then smoothed for 31 days.

We depict the characteristics of MHWs such as frequency, duration and intensity from the AMOC_free and AMOC_fx simulations. Frequency is defined as the number of events per year; duration is defined as the time between the start date and end date of the event; and intensity is defined as the maximum intensity of each MHW, i.e., the maximum SST anomaly (SSTA) relative to the seasonally varying climate mean over the duration of the event. We apply the Student's t-test to the difference of the MHW characteristics between two suites of simulations to examine the statistical significance of AMOC impacts on MHWs.

3. Results

We first analyze the global MHWs during the past four decades (1981-2020) in the AMOC_free simulation. We find high-intensity MHWs of long duration mainly in the eastern tropical Pacific (Figure 1a) with an average MHW duration of about 70 days. These MHWs are heavily influenced by ENSO variability (Gupta et al., 2020; Holbrook et al., 2020). We also find short-lived, high-intensity MHWs in the western boundary current extension regions (e.g., the Gulf Stream and Kuroshio extension, c.f. Chen et al., 2014; Oliver et al., 2018) with an average duration of only about 40 days. Over a global scale, CCSM4 generally well captures the major characteristics of observed global MHWs during the past four decades (Figure S2). The model, however, simulates an overall longer MHW duration, a lower annual mean MHW frequency and a weaker MHW intensity when compared to observations, which is a common issue in MHW simulations by non-eddy-resolving models (Pilo et al. 2019). Here, we also conjecture that the discrepancy between model and observation stems from the fact that in observation the daily SST climatology results from this sole realization. While in model a five-member ensemble mean daily SST climatology is employed for MHW detections in different ensemble members so that some short-duration MHWs are difficult to be determined or potentially mixed with intense long-duration MHWs. This discrepancy, however, does not affect our study of AMOC impacts on MHWs. Moreover, the ensemble approach in model simulations helps minimize the effect of climate variability and allows for a better representation of daily SST climatology in a warming climate.

We then compare the global MHWs between the AMOC_free and AMOC_fx simulations to assess the effect of AMOC slowdown on MHWs (Figure 1). During the past four decades, the weakened AMOC leads to a reduction in MHW duration and intensity generally over a global scale (Figure 1c,i), whilst the extent of reduction could be affected by model biases in MHW simulations especially in the western boundary current regions where mesoscale eddies are pivotal in driving SST extremes (Pilo et al. 2019). The weakened AMOC also helps diminish the frequency of MHWs in the Northern Hemisphere, but enhance the frequency of those in the Southern Hemisphere (Figure 1f), which is akin to a so-called "bipolar seesaw" pattern (Stocker and Johnsen 2003; Rathore et al. 2020). The AMOC induced changes in MHWs are generally insignificant when compared to the changes due to natural climate variability. This is likely owing to the relatively small amplitude of AMOC slowdown during this period (Figure S1b). One exception occurs in the North Atlantic to the south of Greenland where ocean circulation plays an essential role in modulating SST (Li et al., 2020). In this so-called North Atlantic warming hole (NAWH) region (Drijfhout et al. 2012; Liu & Federov 2019), the weakened AMOC significantly alters the duration and frequency of MHWs (Figure S3e.f). Particularly, the AMOC slowdown generates a reduced northward oceanic heat transport and hence a net heat transport divergence in the subpolar North Atlantic, resulting in an abated ocean heat storage and a surface warming minimum there (Liu et al., 2020). Under the relative cooler mean-state SST (Figure S3e), the annual average numbers of occurrence and duration of MHWs in the NAWH region have dropped by about half between 1981 and 2020 (Figure 1g,h).

We further investigate the AMOC effect on global MHWs in future climate (Figure 2). During 2061-2100, the AMOC slowdown brings about a decrease in MHW durations in the

Northern Hemisphere but an increase in the Southern Hemisphere (Figure 2c). The AMOC effect is significant over a much broader area than that during 1981-2020—not only in the NAWH region but also in the low latitudes in the Atlantic, the mid- to high-latitudes in the North Pacific and the Arctic—which is likely owing to the larger decline of the AMOC strength towards the end of the twenty-first century (Figure S1b). The weakened AMOC also induces a reminiscent change of bipolar-seesaw in MHW frequency, giving rise to more frequent MHWs in the Southern Hemisphere but less frequent MHWs in the North Hemisphere except over the NAWH (Figure 2c). By the end of the twenty-first century, the NAWH south of Greenland remains the most sensitive area for MHWs to be affected by the AMOC. If the AMOC were not to slow down, the NAWH region would reach a near-permanent MHW state (Oliver et al., 2019) over 2061-2100 in which MHWs would have ultra-long durations (Figure 2b) and reduced annual frequencies (Figure 2e) as well as enlarged magnitudes (Figure 2h).

We further illustrate the AMOC effect on regional warm SST extremes from a perspective of the probability density function (PDF). We select four "hot spots" in the Northern Hemisphere where MHWs have occurred during past decades covering the Gulf of Maine, the northern Mediterranean Sea, the East China Sea and the California Current region, and also, the NAWH that is highly sensitive to AMOC changes (Figure 3a). For each region, we calculate the PDF of daily SSTA that is relative to the daily SST climatology within a referenced period with an interval of 0.1°C. We define the 90th percentile of SSTA PDF to indicate warm extremes or MHWs and compare the SSTA PDFs between the AMOC_free and AMOC_fx simulations to assess the AMOC effect on warming extremes in these regions.

We discover that the weakened AMOC generally has a minor impact on the warm extremes in the historical MHW "hot spots" during 1981-2020 (Figure 3b,d,h,j). Though it induces a small shift (≤0.1°C) in the mode of SSTA PDFs toward their lower tails in the "hot spots", the weakened Atlantic overturning does not markedly alter the shape of SSTA PDFs and hence the likelihood of MHW occurrence in these regions. On the other hand, the weakened AMOC causes a large shift of the PDF towards its lower tail (with a mode displacement by about -0.2°C) for the SSTA over the NAWH, leading to a large reduction of the area under the curve for the PDF beyond the 90th percentile (Figure 3f). This means, via a local mean-state SST cooling (Figure S3), the weakened AMOC diminishes the likelihood of MHW occurrence in the NAWH over the past four decades.

During 2061-2100, the strong AMOC weakening prompts a large shift of SSTA PDFs towards their lower tails and hence a reduction in the likelihood of MHW occurrence in all five regions, especially over the NAWH (Figure 3c,e,g,i,k). This result is consistent with the bipolar-seesaw like change in global MHW frequency in our previous analysis (Figure 2f) and highlights the significant AMOC impact on MHW frequency in the North Atlantic and Pacific Oceans by the end of the twenty-first century.

Besides, we explore the evolution patterns of global average of MHW characteristics during 1981-2020 and 2061-2100. The global MHWs in the AMOC_free simulation show an overall trend of longer duration, higher frequency and stronger intensity during the past four decades (Figure 4a,c,e) primarily due to the influence of anthropogenic warming (Figure S3a-d, also c.f. Frölicher et al., 2018; Laufkötter et al., 2020). On the other hand, the AMOC_fx simulation shows highly similar evolution patterns of MHW duration, frequency and intensity to those in the AMOC_free simulation, indicative of an insignificant impact of AMOC slowdown on most MHWs over global oceans during this period (Figure 4a,c,e). However, as the AMOC continues weakening, its impacts on MHWs become significant from the global mean perspective. During 2061-2100, the global averages of MHW duration, frequency and intensity in the AMOC_fx simulation are generally much larger than those in the AMOC_free simulation (Figure 4b,d,f). For instance, if the AMOC were not to weaken during the twenty-first century, the average duration of global MHWs will prolong by 10-35 days. Most of this AMOC impact comes from the Northern Hemisphere (Figure S4) instead of the Southern Hemisphere (Figure S5). It also merits attention that the AMOC impact on MHW frequency seems muted after mid-2080s when the average frequency of global MHWs in the AMOC_fx simulation gets very close to that in the AMOC_free simulation (Figure 4e). This result can be explained by the near-permanent MHW state over the NAWH if there were to be a lack of AMOC slowdown, which would induce a local decrease of MHW frequency compensating the increase of MHW frequency in many other regions in the Northern Hemisphere (Figure 2e).

4. Summary and Conclusions

In this study, we have analyzed the global MHW characteristics since 1980s and explored the effect of centurial AMOC slowdown on MHWs in the context of global warming by controlling the AMOC strength through CCSM4 experiments. We find that the AMOC slowdown leads to a reminiscent change of bipolar-seesaw in global MHW frequency, appearing as less and more frequent MHWs in the Northern and Southern Hemispheres. Compared to natural climate variability, the AMOC effect on MHWs is insignificant during the past four decades over the global oceans except in the NAWH region where the weakened AMOC leads to a divergence of meridional oceanic heat transport and a relative cooler mean-state SST, helping cut the annual occurrence and duration of MHWs by about half. This feature is further illustrated by the PDF changes of regional SSTAs. Accompanying with a continuous AMOC slowdown in the current century, the AMOC effect on MHWs becomes significant over a much broader area in the Northern Hemisphere during 2061-2100, which covers the Gulf of Maine, the northern Mediterranean Sea, the East China Sea and the California Current region. The NAWH region would reach a near-permanent MHW state if the AMOC were not to weaken, which would lead to a local decrease of MHW frequency against the increase of MHW frequency in many other regions in the Northern Hemisphere. As a result, the global averages of MHW frequency are highly similar between the AMOC_free and AMOC_fx simulations.

Above results are based on 1-degree CCSM4 simulations. Nevertheless, it has been suggested that high-resolution climate models with with 0.1-degree oceans could better represent temperature changes in coastal regions (e.g., Saba et al., 2016) and also likely better simulate AMOC structure (Hirschi et al., 2020). It has also been shown that the model of 0.1-degree ocean exhibits improvements in global and regional MHW simulations when compared with the model of 1-degree ocean (Pilo et al. 2019). To this end, the AMOC impact on global MHWs is expected to be further tested using high-resolution climate models.

Acknowledgments and data

This work is supported by grants to W.L. from U.S. National Science Foundation (AGS-2053121 and OCE-2123422). W.L. is also supported by the Alfred P. Sloan Foundation as a Research Fellow and by the Hellman Fellows Fund as a Hellman Fellow. We would like to thank Neil Holbrook and another anonymous reviewer for their insightful reviews. We also would like to thank Jian Zhao for beneficial discussions. The OISST v2.1 data are available at https://www.ncdc.noaa.gov/oisst/optimum-interpolation-sea-surface-temperature-oisst-v21 The calculation of MHW intensity, duration and frequency follows Oliver et al. (2018) and Holbrook, et al. (2019), and the code for calculation is available at https://github.com/ecjoliver/MHW_Drivers
Data of CCSM4 and other CMIP5 historical and RCP8.5 simulations are available at https://esgf-node.llnl.gov/projects/cmip5/
The AMOC_fx experiment is performed by modifying the source code of CCSM4 based on Liu et al. (2020), and the source code of CCSM4 is available at https://www.cesm.ucar.edu/models/ccsm4.0/
The data to generate Figures 1-4 are available at zenodo. DOI: 10.5281/zenodo.5559774

References

1. Amaya, D.J., Miller, A.J., Xie, S.-P., & Kosaka, Y. (2020), Physical drivers of the summer 2019 North Pacific marine heatwave, Nat. Commun., 11, 1903.
2. Banzon, V., Smith, T.M., Steele, M., Huang, B., & Zhang, H.-M. (2020), Improved estimation of proxy sea surface temperature in the Arctic, J. Atmos. Ocean. Technol., 37, 341-349.
3. Bensoussan, N., Romano, J.C., Harmelin, J.G., & Garrabou, J. (2010), High resolution characterization of northwest Mediterranean coastal waters thermal regimes: to better understand responses of benthic communities to climate change, Estuar. Coast. Shelf Sci., 87, 431–441.
4. Benthuysen, J.A., Feng, M., & Zhong, L. (2014), Spatial patterns of warming off Western Australia during the 2011 Ningaloo Niño: quantifying impacts of remote and local forcing, Cont. Shelf Res., 91, 232–246.
5. Bond, N.A., Cronin, M.F., Freeland, H., & Mantua, N. (2015), Causes and impacts of the 2014 warm anomaly in the NE Pacific, Geophys. Res. Lett., 42, 3414–3420.
6. Chen, K., Gawarkiewicz, G.G., Kwon, Y.-O., & Zhang, W.G. (2015), The role of atmospheric forcing versus ocean advection during the extreme warming of the northeast U.S. continental shelf in 2012, J. Geophys. Res. Oceans, 120, 4324–4339.
7. Chen, K., Gawarkiewicz, G.G., Lentz, S.J., & Bane, J.M. (2014), Diagnosing the warming of the northeastern U.S. coastal ocean in 2012: a linkage between the atmospheric jet stream variability and ocean response, J. Geophys. Res. Oceans, 119, 218–227.
8. Di Lorenzo, E., & Mantua, N. (2016), Multi-year persistence of the 2014/15 North Pacific marine heatwave, Nat. Clim. Change, 6,1042–1047.

9. Drijfhout, S., Van Oldenborgh, G.J., & Cimatoribus, A. (2012), Is a decline of AMOC causing the warming hole above the North Atlantic in observed and modeled warming patterns?, J. Clim., 25, 8373-8379.
10. Feng, M., McPhaden, M., Xie, S.-P., & Hafner, J. (2013), La Niña forces unprecedented Leeuwin Current warming in 2011, Sci. Rep., 3, 1277.
11. Frajka-Williams, E. (2015), Estimating the Atlantic overturning at 26°N using satellite altimetry and cable measurements, Geophys. Res. Lett., 42, 3458–3464.
12. Frölicher, T.L., Fischer, E.M., & Gruber, N. (2018), Marine heatwaves under global warming, Nature, 560, 360-364.
13. Garrabou, J., Coma, R., Bensoussan, N., Bally, M., Chevaldonné, P., Cigliano, M., et al. (2009), Mass mortality in Northwestern Mediterranean rocky benthic communities: effects of the 2003 heat wave, Glob. Change Biol., 15, 1090-1103.
14. Gent, P.R., Danabasoglu, G., Donner, L.J., Holland, M.M., Hunke, E.C., Jayne, S.R., et al. (2011), The community climate system model version 4, J. Clim., 24, 4973-4991.
15. Greene, C.H. (2016), North America's iconic marine species at risk due to unprecedented ocean warming, Oceanogr., 29,14–17.
16. Gupta, A.S., Thomsen, M., Benthuysen, J.A., Hobday, A.J., Oliver, E., Alexander, L.V., et al. (2020), Drivers and impacts of the most extreme marine heatwave events, Sci. Rep., 10, 1-15.
17. Hirschi, J.J.M., Barnier, B., Böning, C., Biastoch, A., Blaker, A.T., Coward, A., et al., (2020), The Atlantic meridional overturning circulation in high-resolution models, J. Geophys. Res.: Oceans, 125, e2019JC015522.
18. Hobday A.J., Alexander, L.V., Perkins, S.E., Smale, D.A., Straub, S.C., Oliver, E.C., et al. (2016), A hierarchical approach to defining marine heatwaves, Prog. Oceanogr., 141, 227–238.
19. Holbrook, N.J., Scannell, H.A., Gupta, A.S., Benthuysen, J.A., Feng, M., Oliver, E.C., et al. (2019), A global assessment of marine heatwaves and their drivers, Nat. Commun., 10, 2624.
20. Holbrook, N.J., Sen Gupta, A., Oliver, E.C.J., Hobday, A.J., Benthuysen, J.A., Scannell, H.A., et al. (2020), Keeping Pace with Marine Heatwaves, Nat. Rev. Earth Environ., 1, 482-493.
21. Holbrook, N.J., D.C. Claar, A.J. Hobday, K.L. McInnes, E.C.J. Oliver, A. Sen Gupta, et al. (2021), ENSO-driven ocean extremes and their ecosystem impacts. Chapter 18 (pp 409-428) In: ENSO in a Changing Climate (Eds. MJ McPhaden, A Santoso and W Cai), American Geophysical Union (AGU), https://doi.org/10.1002/9781119548164.ch18.
22. Huang, B., Liu, C., Banzon, V., Freeman, E., Graham, G., Hankins, B., et al. (2021a), Improvements of the Daily Optimum Sea Surface Temperature (DOISST) - Version 2.1, J. Clim., 34, 2923-2939.
23. Huang, B., Liu, C., Freeman, E., Graham, G., Smith, T., & Zhang, H.-M. (2021b), Assessment and intercomparison of NOAA Daily Optimum Interpolation Sea Surface Temperature (DOISST) Version 2.1, J. Clim., 34, 7421-7441.
24. Jacox, M.G., Hazen, E.L., Zaba, K.D., Rudnick, D.L., Edwards, C.A., Moore, A.M., et al. (2016), Impacts of the 2015–2016 El Niño on the California Current System: Early assessment and comparison to past events, Geophys. Res. Lett., 43, 7072–7080.
25. Krumhardt, K. M., Lovenduski, N. S., Long, M. C., & Lindsay, K. (2017), Avoidable impacts of ocean warming on marine primary production: Insights from the CESM ensembles, Global Biogeochem. Cycles, 31, 114–133.
26. Laufkötter, C., Zscheischler, J., & Frölicher, T.L. (2020), High-impact marine heatwaves attributable to human-induced global warming, Science, 369,1621-1625.

27. Li, L., Lozier, M.S., & Buckley, M.W. (2020), An investigation of the ocean's role in Atlantic multidecadal variability, J. Clim., 33, 3019-3035.
28. Liu, W., Xie, S.-P., Liu, Z., & Zhu, J. (2017), Overlooked possibility of a collapsed Atlantic Meridional Overturning Circulation in warming climate, Sci. Adv., 3, e1601666.
29. Liu, W., & Fedorov, A.V. (2019), Global impacts of Arctic sea ice loss mediated by the Atlantic meridional overturning circulation, Geophys. Res. Lett., 46, 944–952.
30. Liu, W., Fedorov, A.V., Xie, S.-P., & Hu, S. (2020), Climate impacts of a weakened Atlantic Meridional Overturning Circulation in a warming climate, Sci. Adv., 6, eaaz4876.
31. Mills, K.E., Pershing, A.J., Brown, C.J., Chen, Y., Chiang, F.-S., Holland, D., et al. (2013), Fisheries management in a changing climate: lessons from the 2012 ocean heat wave in the Northwest Atlantic, Oceanography, 26, 191–195.
32. Maloney, E.D., & Kiehl, J.T. (2002), MJO-related SST variations over the tropical eastern Pacific during Northern Hemisphere Summer, J. Clim., 15, 675–689.
33. Oliver, E.C.J., Benthuysen, J.A., Bindoff, N.L., Hobday, A.J., Holbrook, N.J., Mundy, C.N., et al. (2017), The unprecedented 2015/16 Tasman Sea marine heatwave, Nat. Commun., 8, 16101.
34. Oliver, E.C.J., Benthuysen, J.A., Darmaraki, S., Donat, M.G., Hobday, A.J., & Holbrook, N.J. (2021), Marine Heatwaves, Ann. Rev, Mar. Sci., 13, 313-342.
35. Oliver, E.C., Burrows, M.T., Donat, M.G., Sen Gupta, A., Alexander, L.V., Perkins-Kirkpatrick, S.E., et al. (2019), Projected marine heatwaves in the 21st century and the potential for ecological impact, Front. Mar. Sci., 6, 734.
36. Oliver E.C.J., Donat M.D., Burrows, M.T., Moore, P.J., Smale, D.A., Alexander, L.V., et al. (2018), Longer and more frequency marine heatwaves over the past century, Nat. Commun., 9, 1324.
37. Pershing, A.J., Alexander, M.A., Hernandez, C.M., Kerr, L.A., Le Bris, A., Mills, K.E., et al. (2015), Slow adaptation in the face of rapid warming leads to collapse of the Gulf of Maine cod fishery, Science, 350, 809-812.
38. Peterson, W.T., Fisher, J.L., Strub, P.T., Du, X., Risien, C., Peterson, J., et al. (2017), The pelagic ecosystem in the Northern California Current off Oregon during the 2014–2016 warm anomalies within the context of the past 20 years, J. Geophys. Res. Oceans, 122, 7267– 7290.
39. Rahmstorf, S., Box, J.E., Feulner, G., Mann, M.E., Robinson, A., Rutherford, S., et al. (2015), Exceptional twentieth-century slowdown in Atlantic Ocean overturning circulation, Nat. Clim. Change, 5, 475–480.
40. Rathore, S., Bindoff, N.L., Phillips, H.E., & Feng M. (2020), Recent hemispheric asymmetry in global ocean warming induced by climate change and internal variability, Nat. Commun. 11, 2008.
41. Saba, V.S., Griffies, S.M., Anderson, W.G., Winton, M., Alexander, M.A., Delworth, T.L., et al. (2016), Enhanced warming of the Northwest Atlantic Ocean under climate change, J. Geophys. Res. Oceans, 121, 118–132.
42. Scannell, H.A., Pershing, A.J., Alexander, M.A., Thomas, A.C., & Mills, K.E. (2016), Frequency of marine heatwaves in the North Atlantic and North Pacific since 1950, Geophys. Res. Lett., 43, 2069–2076.
43. Schlegel, R.W., Oliver, E.C., & Chen, K. (2021), Drivers of Marine Heatwaves in the Northwest Atlantic: The Role of Air–Sea Interaction During Onset and Decline, Front. Mar. Sci., 8. 627970.
44. Smale, D.A., Wernberg, T., Oliver, E.C., Thomsen, M., Harvey, B.P., Straub, S.C., et al. (2019), Marine heatwaves threaten global biodiversity and the provision of ecosystem services, Nat. Clim. Change, 9, 306-312.

45. Smeed, D. A., Josey, S.A., Beaulieu, C., Johns, W.E., Moat, B.I., Frajka-Williams, E., et al. (2018), The North Atlantic Ocean is in a state of reduced overturning, Geophys. Res. Lett., 45, 1527–1533.
46. Stocker, T.F., & Johnsen, S.J. (2003), A minimum thermodynamic model for the bipolar seesaw, Paleoceanography, 18, 1087.
47. Tan, H., & Cai, R. (2018), What caused the record-breaking warming in East China Seas during August 2016?, Atmos. Sci. Lett., 19, 853.
48. Thornalley, D.J.R., Oppo, D.W., Ortega, P., Robson, J., Brierley, C.M., Davis, R., et al. (2018), Anomalously weak Labrador Sea convection and Atlantic overturning during the past 150 years, Nature, 556, 227-230.
49. Weaver, A.J., Sedláček, J., Eby, M., Alexander, K., Crespin, E., Fichefet, T., et al. (2012), Stability of the Atlantic meridional overturning circulation: A model intercomparison, Geophys. Res. Lett., 39, L20709.

Figures

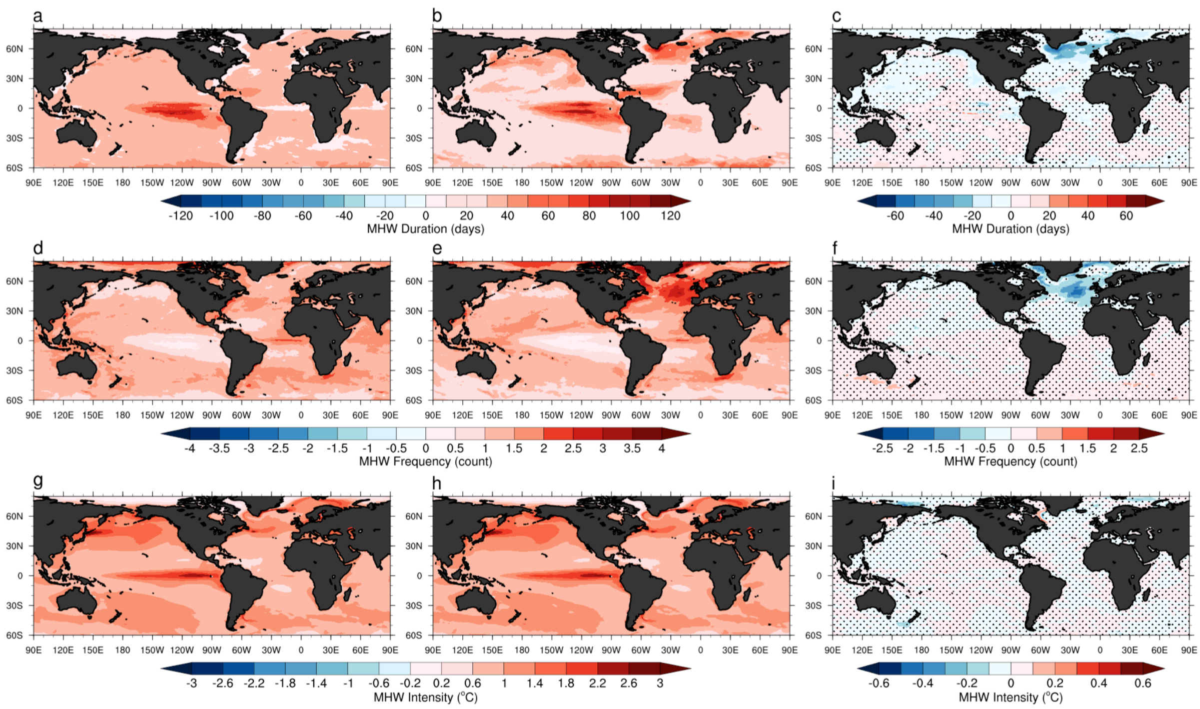

Figure 1. (top row) Durations of global marine heatwaves (MHWs) for the ensemble means of CCSM4 (a) AMOC_free and (b) AMOC_fx simulations during 1981–2020 as well as (c) the difference between the two (a minus b). (middle row) Similar to the top row but for annual mean MHW frequencies. (bottom row) Similar to the top row but for MHW intensities. Dotted indicates that the change is not significantly different from zero at the 95% level.

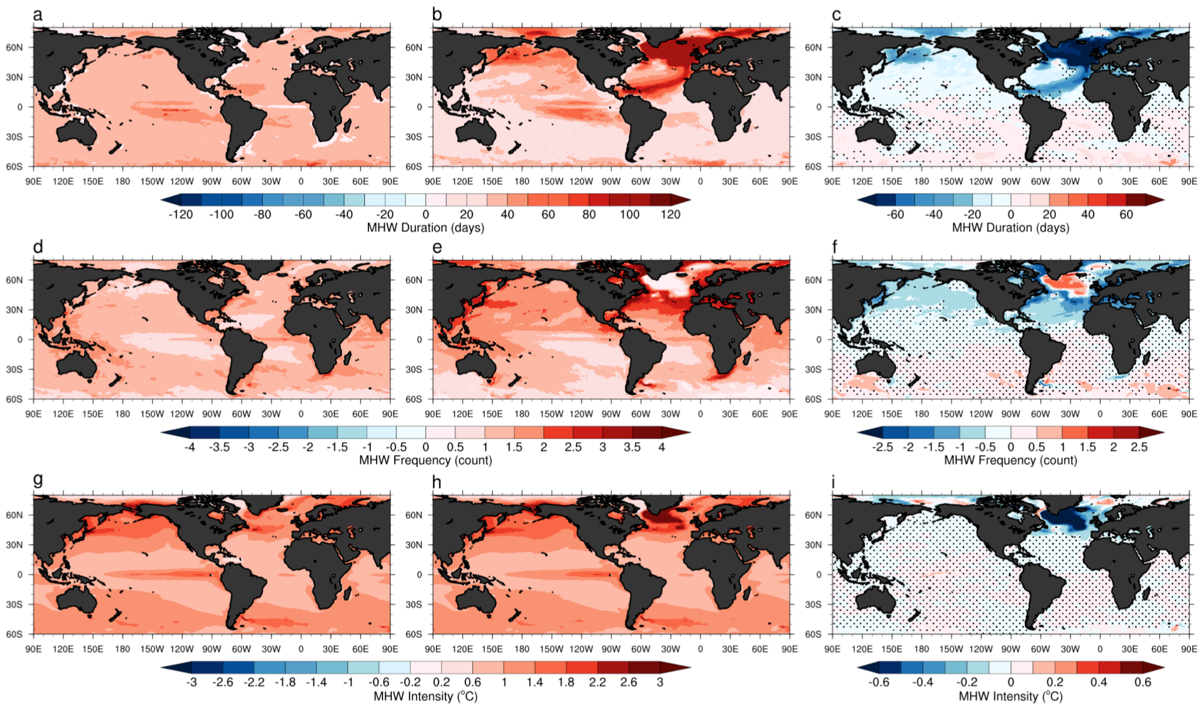

Figure 2. Simiar to Figure 1 but for the period of 2061-2100.

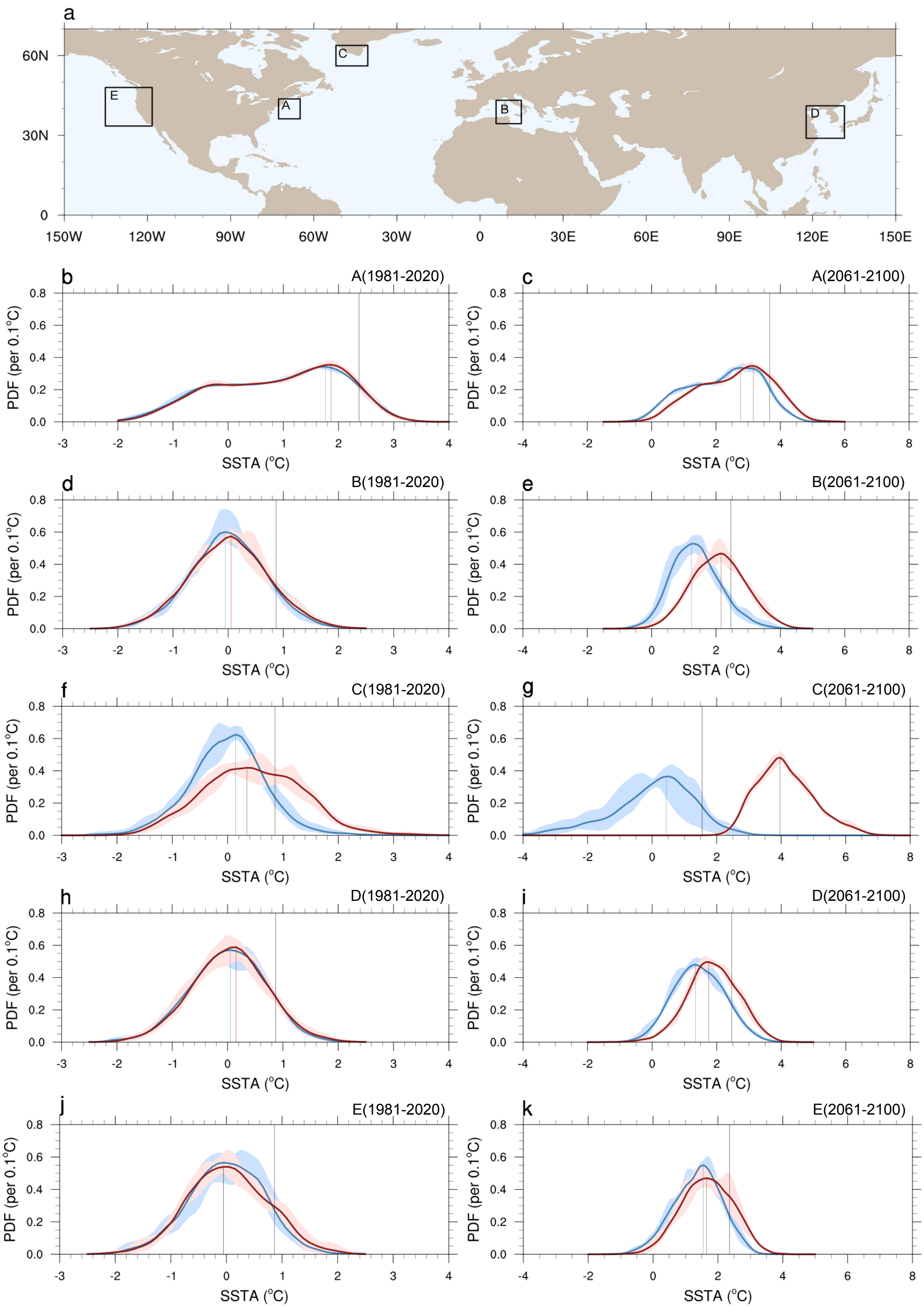

Figure 3. (a) Four "hot spots" of historical MHWs covering [A] the Gulf of Maine, [B] the northern Mediterranean Sea, [D] the East China Sea and [E] the California Current region as well as [C] the North Atlantic warming hole (NAWH) region. (b-k) Probability density functions (PFDs) of sea surface temperature anomaly (SSTA) in these regions during the

periods of (b,d,f,h,j) 1981-2020 and (c,e,g,i,k) 2061-2100 from CCSM4 AMOC_free (ensemble mean, blue solid; mode of the ensemble PDF, blue dashed; ensemble spread, light blue shading) and AMOC_fx (ensemble mean, red solid; mode of the ensemble PDF, red dashed; ensemble spread, light red shaing) simulations. For each region, the SSTA is relative to daily SST climatology during either period. The ensemble spread is calculated as one standard derviation of ensemble members. The 90th percentile of the PDF from the AMOC_free simulation is denoted by gray dashed line.

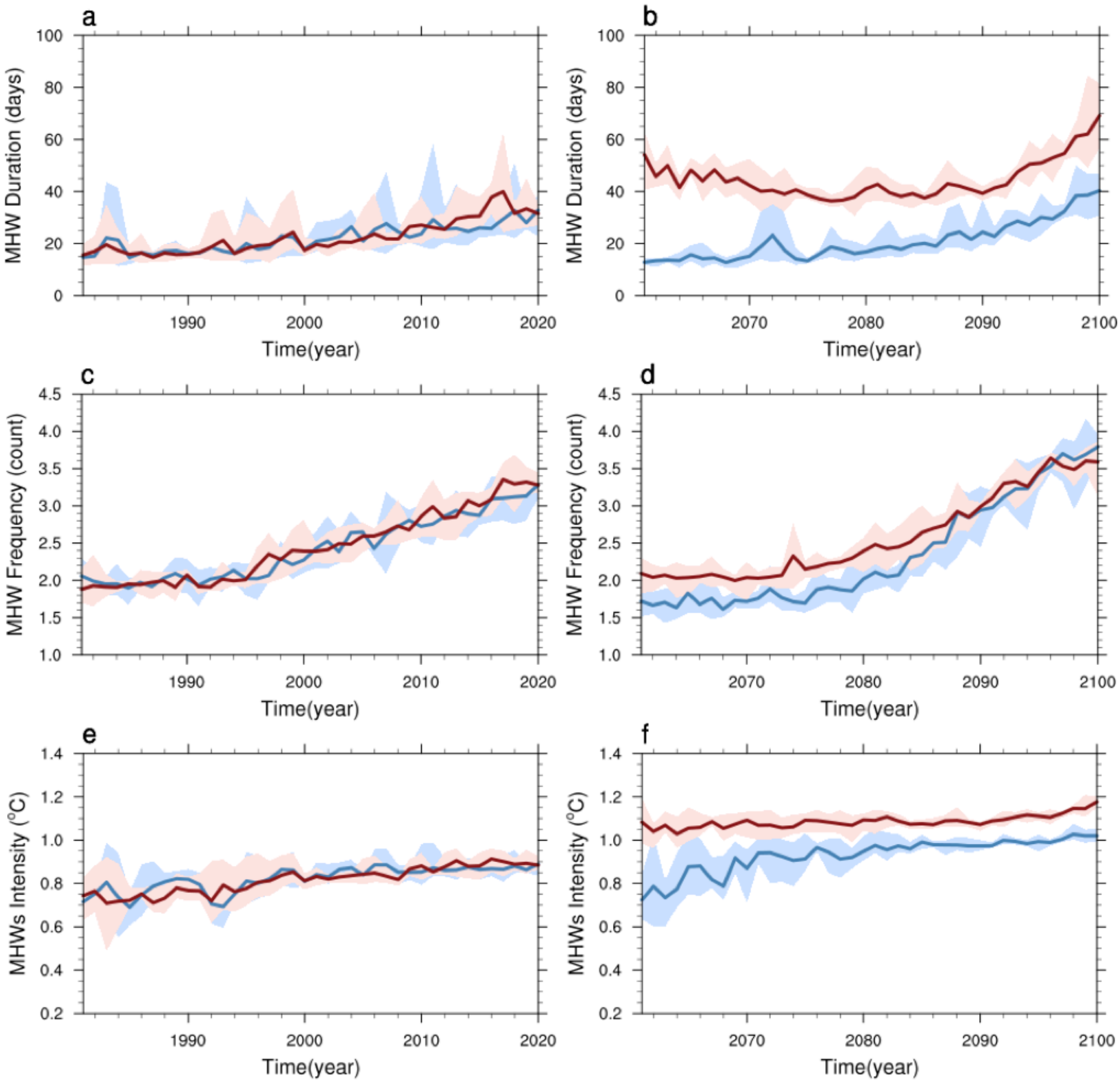

Figure 4. (top row) Global averages of MHW duration from CCSM4 (a) AMOC_free (ensemble mean, blue solid; ensemble spread, light blue shading) and (b) AMOC_fx (ensemble mean, red solid; ensemble spread, light red shading) simulations during 1981–2020. (middle row) Similar to the top row but for global averages of annual mean MHW frequency. (bottom row) Similar to the top row but for global averages of MHW intensity. The ensemble spread is calculated as one standard derviation of ensemble members.